DEVELOPMENT OF INPUT & OUTPUT STRUCTURES FOR HIGH POWER X-BAND TWT AMPLIFIERS *

S. Naqvi, Cz. Golkowski, G. S. Kerslick, J. A. Nation and L. Schächter, Laboratory of Plasma Studies & School of Electrical Engineering, Cornell University, Ithaca, NY 14853, USA

Abstract

Our recent research into multi-stage X-Band TWT amplifiers producing output powers of $100 - 200\ MW$ has shown that it is essential to minimize the reflections in each stage of the amplifier in order to avoid sideband development. These reflections also cause fluctuations in the RF output power envelope. One solution to this problem is to isolate the two stages of the amplifier. Following extensive PIC code simulations and analytical work we have designed the first amplifier stage to provide beam modulation over a range ($\sim 200MHz$) of input frequencies. The second stage is a quasi-periodic structure designed to minimize reflections, and allow the radial or longitudinal RF power extraction to be distributed over an extended region. A second approach uses tapers that adiabatically reduce the loading in the output sections of the amplifier to provide a smooth, broad-band transition from the slow-wave structure to cylindrical waveguide. We are also developing mode converters that will allow extraction in TEM and subsequently in a TE mode of rectangular waveguide.

I. INTRODUCTION

Recent experiments, seeking to optimize the RF input sections of high power TWT amplifiers, have shown significant reductions in efficiency due to beam loading and reflections at impedance mismatches. As a result of these observations we are developing an two-stage amplifier in which the first stage is independently tuneable under vacuum conditions. The input section consists of two waveguide feeds separated by a short section of slow wave structure. RF power is fed into one arm, beam modulation is produced in the structure and the reflections minimized by coupling RF from the system via the output arm. The degree of beam modulation can be increased by passing the beam through additional, passive structures, separated from the input stage by a drift region which is beyond cutoff. Once tuned, the input structure bandwidth is sufficient to accommodate beam detuning, and any reflections at adjacent frequencies are not significant to the interaction.

A second method of reducing reflections in TWT amplifiers uses coupled cells that are tapered to provide a broad-band transition from the slow wave structure to a cylindrical waveguide. MAGIC simulations show that such transitions, if properly designed, can provide efficient power coupling in a coaxial extraction geometry.

*Work supported by US Dept. of Energy

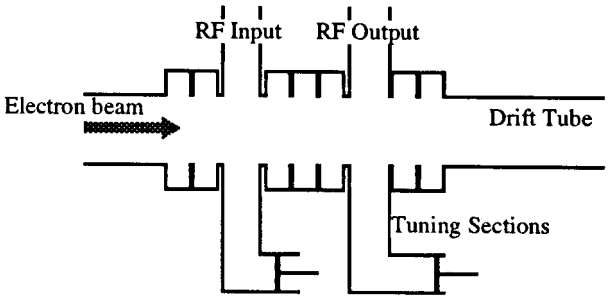

Figure. 1. Tuneable first stage of TWT amplifier.

II. TWT AMPLIFIER INPUT STRUCTURE DESIGN

The input structure has been designed, using an analytical code written at our laboratory, to maximize the input bandwidth while maintaining a useful gain to produce the desired beam modulation. This should significantly reduce problems due to electromagnetic feedback at frequencies close to the design frequency. The structure has a phase advance per cell of $\pi/2$ at an operating frequency of $9GHz$ for an $850kV$ beam. With these parameters each cell has a period, $L = 7.7mm$ a coupling iris length, $d = 1.0mm$ an outer radius, $R_{ext} = 15.3mm$ and an inner radius $R_{int} = 9.0mm$. Note that the output tube connected to the structure also has $R_{int} = 9.0mm$ which has a cutoff frequency of $12.7GHz$ for the TM_{01} mode. The calculated gain is $2.6dB/cm$ or approximately $2dB$ per cell, with a transmission bandwidth of $\sim 200MHz$. This is in contrast to our previous input stages, where the transmission characteristics were limited, by reflections, to a series of narrow transmission peaks, typically separated by tens of MHz, that allowed the development of unwanted sidebands. A schematic of the vacuum tuneable structure is shown in fig.1

The input structure operation has been simulated using the MAGIC code and while the full 3-D nature of the problem can not be modeled some characteristics can be determined. Based on output from the analytical code many configurations were simulated, until the setup shown in fig. 1 was found to show the most promise. The modulation produced on an $850kV, 500A$ beam was examined for a range of input frequencies. This short structure is capable of producing a 7% modulation on the beam for $100kW$ input power. We are currently running simulations on longer structures with the aim of increasing this. The transmission is essentially 100% at $9.08GHz$, and for an input power of $100kW$ the E_z field on axis is $\approx 1.75MV/m$. In numerous simulations the transmission efficiency remains good on both sides of this frequency but the net power injected drops, giving a $3dB$ transmission bandwidth of $\approx 200MHz$.

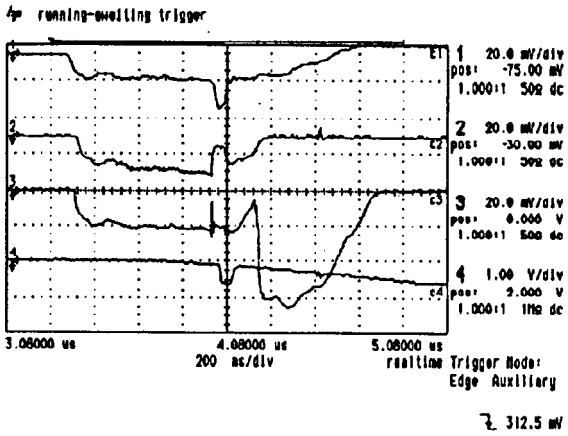

Figure. 2. Microwave waveforms

III. INPUT STRUCTURE RESULTS

The *cold* passband and tuning characteristics have been measured using a network analyzer for a number of cell configurations. The best tuning characteristic, with the maximum transmission bandwidth is obtained with an odd number of cells between the input arm and the output arm.

The transmission and return loss for the $2-3-2$ configuration have been measured using an X-Band magnetron. At the tuned frequency the peak transmission is $-0.86dB$, i.e. 82% of the input power is coupled through the output arm, with a $3dB$ width of $\approx 100MHz$. The return loss at this frequency is $-23.4dB$, i.e. less than 1% of the input power is reflected.

The input structure has been operated using a $850kV, 500A, 50ns$ electron beam and initial results are encouraging. Figure 2 shows the input signal combined with the $50ns$ diode voltage pulse (*top trace*). Trace 2 is the signal transmitted along the output waveguide, showing the power absorbed during beam passage through the slow wave structure. Trace 3 shows the signal reflected from the structure. The level of this signal does not change significantly until $100ns$ after the beam pulse. Trace 4 shows the beam current measured by a Rogowski coil located in the drift tube $25cm$ beyond the slow wave structure.

The signal from an output horn attached to the structure by a $25cm$ length of drift tube, which is cutoff at this frequency, shows that beam modulation has been achieved. As the modulated beam propagates through the non-adiabatic tube-horn transition the RF signal is reconstructed from the space charge modulated beam. The measured signal is heterodyned with a fixed frequency local oscillator. The FFT of this mixed signal shows that the output is single frequency and follows the input magnetron frequency over the full $8.9 - 9.1GHz$ bandwidth of the input structure.

IV. TAPERED SLOW-WAVE STRUCTURES

An extensive study using the MAGIC simulation code has shown that reflections in all stages of an amplifier can be minimized by using correctly designed tapered transition sections. These tapers provide broad-band transitions to a circular TM_{01} mode, and the reduction in reflections also minimizes fluctuations in the output power level. The phase velocity increases from less than c in the slow-wave structure to greater than c in the uniform circular guide. At some point within the tapered region, the phase velocity equals c and close to that point, a coaxial inner conductor can be placed to extract the RF power. Once the beam is within this conductor, it does not interact with the RF flowing in the TEM mode of the coaxial line and can be safely dumped anywhere within the inner conductor. The results of one MAGIC simulation using a $830kV, 550A$ beam are presented in fig. 3. Electron trajectories are shown as the pencil beam propagates through the tapered slow wave structure and into a cylindrical beam dump that is cutoff to the RF signal. The beam enters the left boundary with a $25kV$ voltage modulation. Following the interaction region the axial Poynting flux (time-averaged over one RF period, and shown as the solid line) shows a power flow of $\sim 50MW$ in a TEM mode in the coaxial extraction section. The peak power can be increased to about $\sim 100MW$ if the input modulation is increased or more cells are added to the structure.

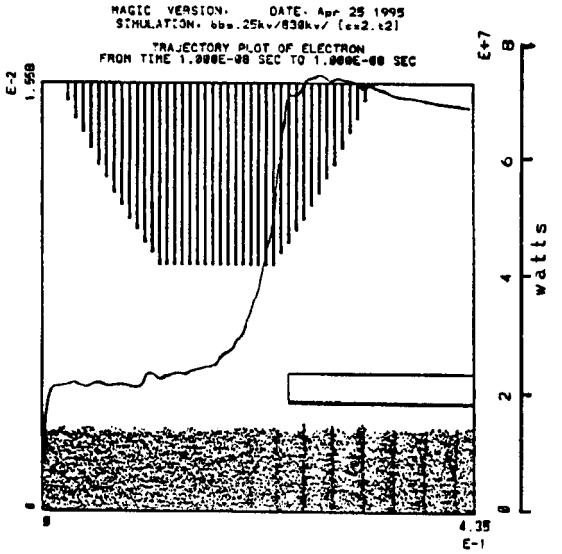

Figure. 3. MAGIC simulation of tapered TWT with coaxial power extraction

V. HIGH EFFICIENCY OUTPUT STRUCTURES

We have investigated the interaction in traveling wave output structures which are expected to generate radiation at an efficiency of 50% and higher. Two different configurations, as described above, are under consideration: (i) Transverse extraction, where the electromagnetic power is extracted perpendicular to the beam flow and therefore an abrupt change in the direction of the power flow is required. Since successful operation requires tuning, the abrupt change in geometry makes this system sensitive to any change in the operation parameters. (ii) Longitudinal extraction, in which case the radiation power is extracted parallel to the beam and the electromagnetic field is gradually decoupled from the beam. This extraction results in the conversion of the TM mode into a TEM mode; at a later stage the TEM can be converted into the TE mode.

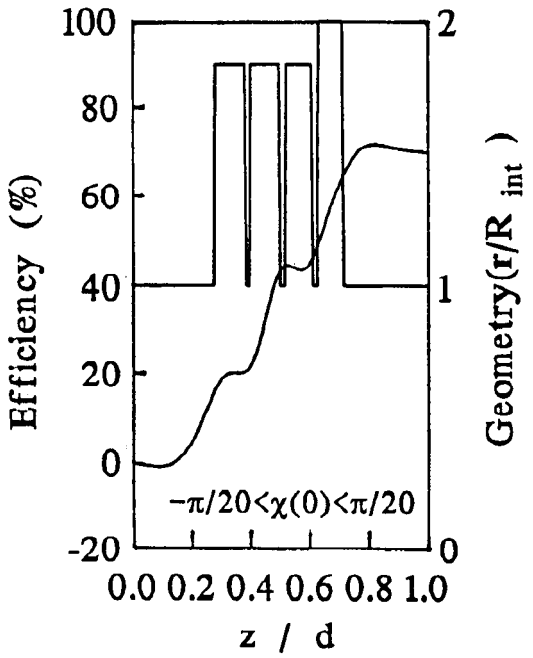

Figure. 4. The variation of the RF conversion efficiency in space for a narrow ($-9^o < \chi(0) < 9^o$) initial phase distribution.

In both configurations we use the formulation of beam-wave interaction in quasi-periodic structures which was developed recently [1], [2]. This is a method which permits analytic calculation of the characteristics of a disk loaded structure with significant variations in the geometry. In principle, once the structure is no longer periodic, the field can not be represented by a single wavenumber. However, in case of adiabatic variations the characteristics of the structure (phase velocity, group velocity and interaction impedance) are assumed to be determined entirely by the geometry of the local cell. This is not the case when significant changes in geometry are required to achieve efficient radiation extraction. This is to say that a non-adiabatic local perturbation of geometry affects *global* electromagnetic characteristics, and a change in a given cell affects the interaction impedance or the group velocity several cells before and after the point where the geometry was altered.

The model consists of a cylindrical waveguide to which a set of pill-box cavities and a radial arm are attached. In principle the number of cavities and arms is arbitrary. The boundary condition problem is formulated in terms of the amplitudes of the electromagnetic field in the cavities and arms. The elements of the matrix which relates these amplitudes with the source term are analytic functions - thus no a-priori knowledge of the functional behavior of the electromagnetic field is necessary. We examined [1] the homogeneous electromagnetic characteristic of quasi-periodic structures; the technique was further developed to include Green's function and the beam-wave interaction within the framework of the linear hydrodynamic approximation for the beam dynamics. It was shown that the method [2] combines the features of the beam-gap (local) interaction, as in a klystron, with those of the beam-wave (distributed) interaction in a traveling wave structure. The linearity of the model above is a serious limitation for a high efficiency interaction, since it is valid only for small variations from the initial average velocity. For this reason, the tools developed previously were used to formulate the beam-wave interaction within the framework of macro-particle dynamics, which permits description of large deviation from average velocity. It was shown that the interaction is controlled by the *matrix interaction impedance*, which can be conceived as a generalization of the scalar interaction impedance concept, used for uniform structures. The design and analysis of a high efficiency (70%) traveling wave section is described in detail elsewhere [3]. Figure 4 shows the RF conversion efficiency in a quasi-periodic output structure, where the cell length decreases from $6.5mm$ in the first cavity to $5.4mm$ in the radial output arm. Results from the formulation of the interaction in the case of longitudinal extraction will be presented elsewhere.

References

[1] L. Schächter and J. A. Nation, *Appl. Phys. Lett.* **63**, 2441 (1993).

[2] L. Schächter and J. A. Nation, *Phys. Plasmas* **2**, 889 (1995).

[3] L. Schächter, submitted for publication in *Phys. Rev. E.*